I. Troch, F. Breitenecker, eds. ISBN 978-3-901608-35-3

CFD MODEL AIDED DESIGN OF PERSONALIZED AIR SUPPLY FOR AIRCRAFT CABIN SEAT

P. Zítek[1], T. Vyhlídal[1], G. Simeunović[1], L. Nováková[2], J. Čížek[2],
[1] Department of Instrumentation and Control Engineering,
Faculty of Mechanical Eng. Czech Technical University in Prague;
[2] Department of Fluid Dynamics and Power Engineering,
Faculty of Mechanical Eng. Czech Technical University in Prague

Corresponding Author: P. Zítek, Department of Instrumentation and Control Engineering,
Faculty of Mechanical Eng. Czech Technical University in Prague,
Technická street 4, 160 00 Prague, Czech republic;
pavel.zitek@fs.cvut.cz

Abstract. The Computer Fluid Dynamics (CFD) model presented in the paper has been developed in the framework of the FP 6 EU Project SEAT where providing an optimal micro-environment for the individual passenger during long-distance commercial flights is one of the project objectives. The presented micro-environment control consists in supplying each of the aircraft passengers with “his/her own” ration of fresh and humidified air with the aim to prevent him/her from possible health problems. Unlike the standard environment control systems commonly used in commercial aircrafts each of the seats in the cabin is considered to be supplied individually with a separated air flow which forms a personalized microclimate in the seat area. Focusing the personal air supply into the breathing area of the passenger is based on the principle of Penot nozzle. The CFD model based design has been verified by means of laboratory experiments.

1 Introduction

At typical cruise altitudes of commercial air transport around 11.000 m, the ambient air temperature is below -50 °C, the atmospheric pressure is five times lower than that at sea level and relative humidity is near to zero. Under these circumstances it is an extremely demanding task to provide acceptable environmental conditions for the passengers in the airplane cabin – by means of the environmental control system (ECS). The most important task of ECS is distributing the properly conditioned air uniformly over the whole aircraft cabin volume. The passenger density in the cabin is much higher than in other transport means and therefore the indispensable air exchange rate is to be extraordinarily high. The air supply is common for the whole cabin and with the aim to maintain reasonable power consumption the internal air is re-circulated – usually in the rate about 50 percent of the whole supply and hence the air-conditioning system supplies the cabin with a mixture of outside fresh air and filtered re-circulated cabin air. Due to the recirculation the internal environment cannot be perfectly cleared of pollutants, particularly CO_2, bacteria, viruses, etc. On the other hand the dryness of outdoor fresh air causes considerable lack of humidity in the cabin. There exist humidifying devices for this purpose, however, their application for the whole cabin through the centralized air-conditioning system would lead to an unacceptably high amount of water to be added into the cabin air and due to this the electronic devices would get into a danger of dew condensation leading to dripping and freezing of moisture on the inner surfaces of the aircraft shell.

The longer lasts the flight the deeper is the humidity deficit caused by the intake of dry outdoor air. The on-board measurements have shown unexpectedly rapid humidity drops: already within only 30 min of flight the drops by more than 35% have been observed – e.g. from at least 47% to 11% RH , [8]. Humidity drops to 5% RH and even lower unavoidably arise during long flights if no humidifying processing is applied [9]. According to [4], low humidity can have direct effects on passenger’s health and comfort, causing e.g. drying of the body surface (mucous membranes and skin), dehydration, lower perception of poor air quality, negative effects on thermal comfort, etc. However, unlike most of the passengers which feel the relative humidity level 30 to 40% as satisfactory, for the electronic devices rather dry air is favourable because of the threat of dew point temperature appearance correspondingly to the extremely low outdoor air temperature

The paper presents an original model-based design of personalized system of air distribution around a single seat in the cabin. Within the framework of the FP 6 EU Project SEAT[1] – among other objectives – a system of individual fresh and humidified air supply for each single seat has been developed on the basis of the Computer Fluid Dynamics (CFD) model.

[1] www.seat-project.org

2 Concept of personalized air distribution.

Our proposal of personalized air circulation within the single seat space was motivated by [2] and is based on the principle of Penot nozzle [3]. Analogously to this nozzle arrangement the aim is to create a local-air pocket around a single seat. To reach a closed local air flow pattern focused onto the breathing area of particular passenger it is necessary to provide specific velocity and temperature conditions and to build in properly designed inlet and outlet nozzles for the additional air supply for each of the seats. However, not only the breathing consumption demand is to be met, it is also necessary to satisfy the strict limitation as to the air velocity near the passenger's face. In any case, to meet the comfort standards, this velocity should not exceed 0.2 m per second. Faster air motion is felt as unpleasant draught by most of the passengers. Under these limitations it resulted from our model studies that the additionally personalized ventilation air flow rate cannot exceed the limit approximately from two to three litres per second for a single passenger. It means that about one third of the whole required air supply per person can be provided by this way. But with regard to proper control of this additional air supply the passengers are breathing almost exclusively this air. Since the ratio of the additional air amount to the whole supply is less than a half it can be provided independently on recirculation – as fresh air only – separately for each passenger. To a significant extent it is then possible to prevent the passengers from breathing contaminated air.

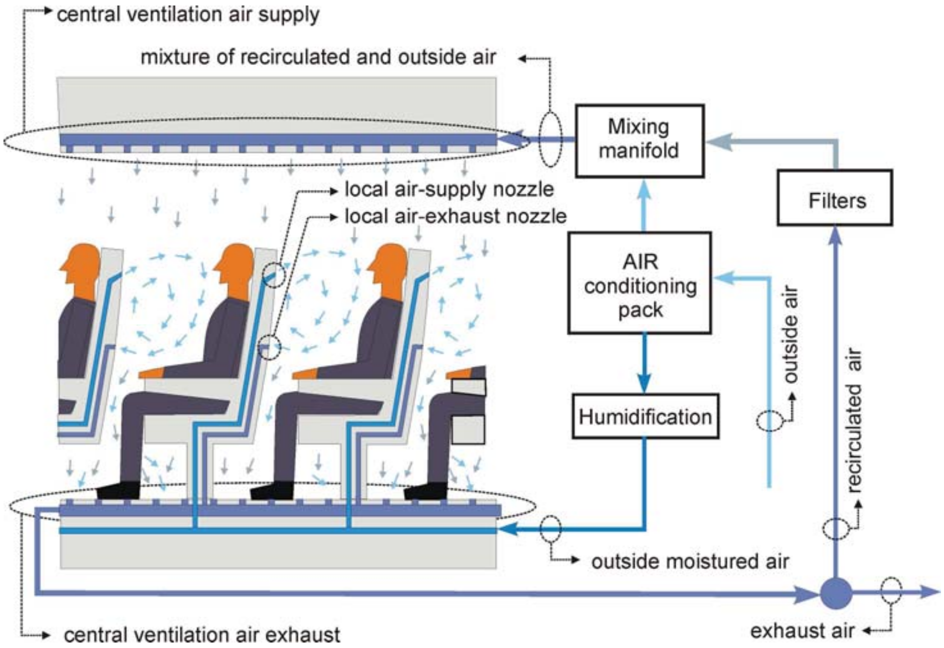

Figure 1 Overall scheme of the personalised air distribution system

Although the additional air circulation affects the breathing area in this way the role of the central air-distribution by ECS remains unchanged – it provides most of the ventilation rate and pressurizes the cabin air as usually. A substantial part of air processed by ECS and supplied to the cabin is recirculated. It is considered in the presented design that – as usually – the central air-supply nozzles are located above the passengers heads at the left and right corners of the cabin below the luggage compartments, while the central-air exhaust nozzles are in the cabin corners at the floor level. As can be seen in Fig. 1, the outside fresh air is processed in the air conditioned pack [1] and the majority of air supply, provided by ECS, passes through the mixing manifold, where it is mixed with the filtered recirculated air. Around 30% of fresh air leaving the air conditioning pack is humidified, preferably using the cold evaporation principle. Then, it is supplied to the seat area by the local air supply nozzles. The air is taken out of the cabin by both local and central ventilation nozzles. Around 50% of this air is exhausted and 50% of it is recirculated. The main role of the personalised local air-distribution system is to supply each passenger with fresh air. Compared to the recirculated air, the fresh air is of lower level of CO_2 and free of contaminants originating from repeatedly breathed air. Moreover, fresh air is supposed to be humidified to the level 20-30% of RH. As can be seen in Fig. 1, both the local air-supply and air-exhaust nozzles are located in the back of the seat ahead.

3 Theoretical Approach to CFD Modelling

The CFD techniques applied in modelling the flow patterns and temperature-humidity distributions became the key tool in investigating the problems of personalized system of single seat environment control. The FLUENT program has been used in implementing the models in all cases [5]. As in [6], the standard $k-\varepsilon$ turbulence model with the heat and humidity transport is applied to describe airflow in the presented models. This turbulence description has been chosen because of its ability to simulate convective heat transfer in buoyancy-driven air flow. The acceptability of the model grid is proved by the *wall-boundary values* y^+ well corresponding with the wall function given as follows

$$y^+ = \frac{\rho u_t y}{\mu} \tag{1}$$

where ρ is air density, μ is the dynamic viscosity, y is the distance from the wall and u_t is the velocity component parallel with the wall.

On the other hand, the standard $k-\varepsilon$ turbulence model provides an acceptable compromise between the grid feasibility and the necessary accuracy of the model. It turned out from the experiments that exaggerated numbers of cells around the passenger are not necessary to achieve the required accuracy and convergence of the solution. Three basic conservation laws – for mass, momentum and energy – are used to describe the air flow pattern inside the aircraft cabin.

3.1 Mass conservation equations

The cabin interior fluid is considered as a mixture of two components, air and water vapour. The mass conservation equation of the mixture consisting of two species, is given by the following equation

$$\frac{\partial(\rho Y_i)}{\partial t} + \nabla(\rho \mathbf{v} Y_i) = -\nabla \mathbf{J}_i \text{ , } i\text{=1,2} \tag{2}$$

where Y_i is the local mass fraction of each component, $\mathbf{v}$ is the velocity vector and $\mathbf{J}_i$ is the diffusion flux of the i-th component. In the turbulent flow the mass diffusion is described by the following equation

$$\mathbf{J}_i = -\left(\rho D_{im} + \frac{\mu_i}{Sc_i}\right)\nabla Y_i \text{ ,} \tag{3}$$

where D_{im} is diffusion coefficient of the i-th component in the mixture, μ_t is turbulent viscosity, and Sc_t is Schmidt number defined by:

$$Sc_t = \frac{\mu_t}{\rho D_t} \text{,} \tag{4}$$

where D_t is the turbulent flow diffusivity.

The convection-diffusion equation (3) is solved for both air and water vapour components. Since the mass fractions of all the components must add up to unity, its sufficient to determine only one mass fraction and the other is then the complement to unity.

3.2 Momentum Conservation Equations of Turbulent Flow. Navier-Stokes equation

The turbulence model parameters, namely kinetic energy rate k, and the dissipation rate ε, are calculated using the following transport equations

$$\frac{\partial(\rho k)}{\partial t} + \frac{\partial(\rho k u_i)}{\partial x_i} = \frac{\partial}{\partial x_i}\left[\left(\mu + \frac{\mu_t}{\sigma_k}\right)\frac{\partial k}{\partial x_j}\right] + G_k + G_b - \rho\varepsilon - Y_M \text{ ,} \tag{5}$$

$$\frac{\partial(\rho \varepsilon)}{\partial t} + \frac{\partial(\rho \varepsilon u_i)}{\partial x_i} = \frac{\partial}{\partial x_j}\left[\left(\mu + \frac{\mu_t}{\sigma_k}\right)\frac{\partial \varepsilon}{\partial x_j}\right] + C_{1\varepsilon}\frac{\varepsilon}{k}(G_k + C_{3\varepsilon}G_b) - C_{2\varepsilon}\frac{\rho\varepsilon^2}{k} \text{ ,} \tag{6}$$

where G_k expresses the generation of turbulence kinetic energy due to the mean velocity gradients defined as

$$G_k = \rho\,\mathrm{m}(u_i' u_j')\frac{\partial u_j}{\partial x_i} \text{ ,} \tag{7}$$

where $\mathrm{m}(u_i' u_j')$ is the *mean value* of the products of i-th and j-th velocity fluctuation components (turbulent share stress), and G_b is the generation of turbulence due to buoyancy given as follows

$$G_b = g\frac{\mu_t}{\rho \Pr_t}\frac{\partial \rho}{\partial x_i} \text{ .} \tag{8}$$

This term is to be taken into account when the gravity field and temperature gradient are present simultaneously. The turbulent viscosity μ_t is defined by

$$\mu_t = \rho C_\mu \frac{k^2}{e} \ , \tag{9}$$

where ρ is air density. The symbols σ_k and σ_ε are used in (5) and (6) for Prandtl numbers appropriate to k and ε respectively [6]. The Prandtl number expresses the distinction between both the velocity and temperature distribution, its values in our case are from 0.7 to 0.9 (the unit value means the same distribution of both). The model constants $C_{1\varepsilon}, C_{2\varepsilon}$ and $C_{3\varepsilon}$ are given in [6]. Particularly $C_{3\varepsilon}$ expressing the influence of buoyancy on the rate of dissipation is given as follows [7]

$$C_{3\varepsilon} = \tanh \frac{v}{u} \tag{10}$$

Where v is velocity component parallel to the gravitational vector and u is velocity component perpendicular to the gravitational vector. The effect of compressibility Y_M on the turbulence in (5) is given by

$$Y_M = 2\rho\varepsilon M_t^2 \tag{11}$$

Where M_t is the Mach number. With regard to a very low value of M_t this term turns out to be negligible.

3.3 Energy Conservation Equations

Taking into account the Reynolds analogy with the turbulent momentum transfer, the modified energy conservation is given by the following equation

$$\frac{\partial(\rho E)}{\partial t} + \frac{\partial[u_i(\rho E + p)]}{\partial x_i} = \frac{\partial}{\partial x_j}\left[k_{eff}\frac{\partial \vartheta}{\partial x_j} + u_i(\tau_{ij})_{eff}\right], \tag{12}$$

where E is the total energy, ϑ is the air temperature, k_{eff} is the effective thermal conductivity and $(\tau_{ij})_{eff}$ is the deviatoric stress tensor.

The deviatoric stress tensor is given by the following equation

$$(\tau_{ij})_{eff} = \mu_{eff}\left(\frac{\partial u_j}{\partial x_i} + \frac{\partial u_i}{\partial x_j}\right) - \frac{2}{3}\mu_{eff}\frac{\partial u_i}{\partial x_i}\delta_{ij} \ , \tag{13}$$

where μ_{eff} is the effective fluid viscosity. The effective thermal conductivity is given as

$$k_{eff} = k + \frac{c_p \mu_t}{\mathrm{Pr}_t} \ , \tag{14}$$

where k is the thermal conductivity, c_p specific heat capacity at constant pressure. The double precision steady state separate solver with second order upwind scheme is used to solving this equation in both models. The iterations used the SIMPLE algorithm to couple the pressure and the velocity with a chosen solver. This algorithm has lower accuracy than PISO but this one has much better convergence ability with grid of lower resolution and with satisfactory accuracy. The standard wall function is applied to describe the influence of the wall on the air flow pattern near the wall.

4 Validation of CFD models

Before the 3D model simulation analysis in FLUENT it is necessary to validate the model on measured data. Taking into account the aircraft cabin dimensions, the validation of the whole aircraft cabin CFD model would be very expensive and experimentally demanding. Thus, for validating the modelling approach, two easier experiments have been performed. First, the model of inlet nozzle profile has been validated followed by validation of the personalized ventilation of a single seat without a passenger.

4.1 CFD model of the inlet nozzle

The inlet nozzle is designed in order to reach as uniform air-velocity profile along the nozzle length as possible. In order to achieve such air-velocity distribution, a set of holes has been placed inside the nozzle in front of the diffuser, see Fig. 2 (the 3D model of the nozzle has been generated in the GAMBIT program). Due to the presence of the small holes inside the nozzle, an unstructured tetrahedral grid has been used for meshing this model as shown in Fig. 3.

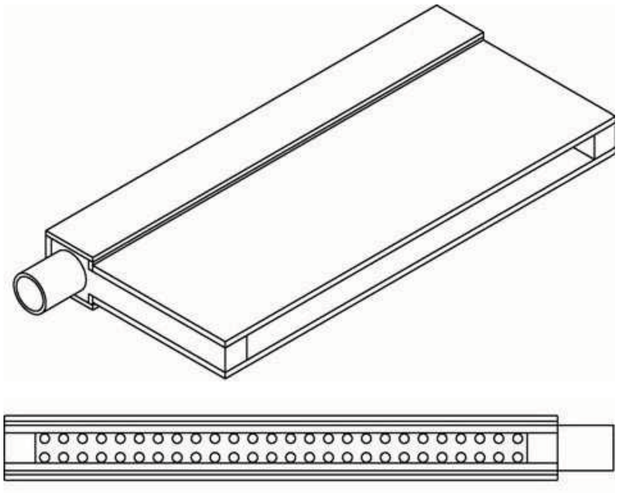

Figure 2 3D model of the inlet (air-supply) nozzle, isometric and top view

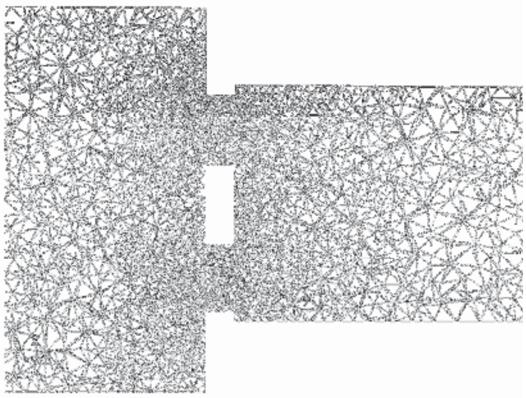

Figure 3 An unstructured tetrahedral grid used for CFD model of the air-supply nozzle

The 3D model has been used for simulations in the FLUENT program. Resulting velocity profile along the nozzle is shown in the Fig. 5 –left. On the basis of the simulation results it is apparent that the velocity profile is uniformly distributed. The velocity profile has been measured by a PIV method (Particle Image Velocimetry), using safex fog for visualisation of the flow patterns. The overal scheme of the experimental set-up is in Fig. 4.

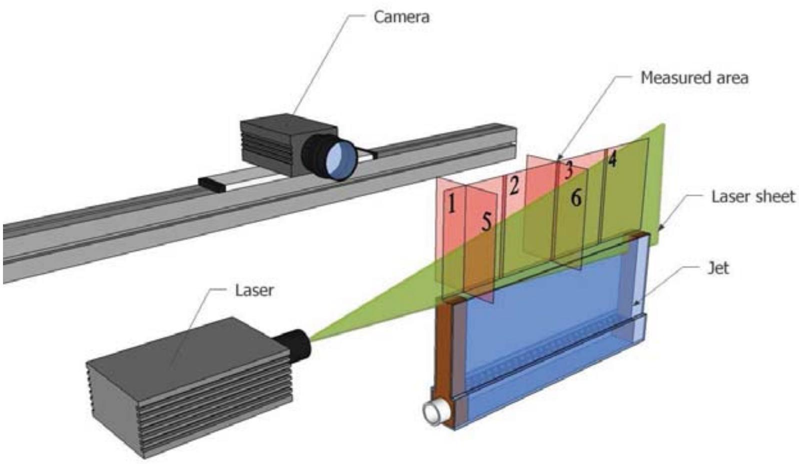

Figure 4 The experimental set-up for validation of the personalised ventilation

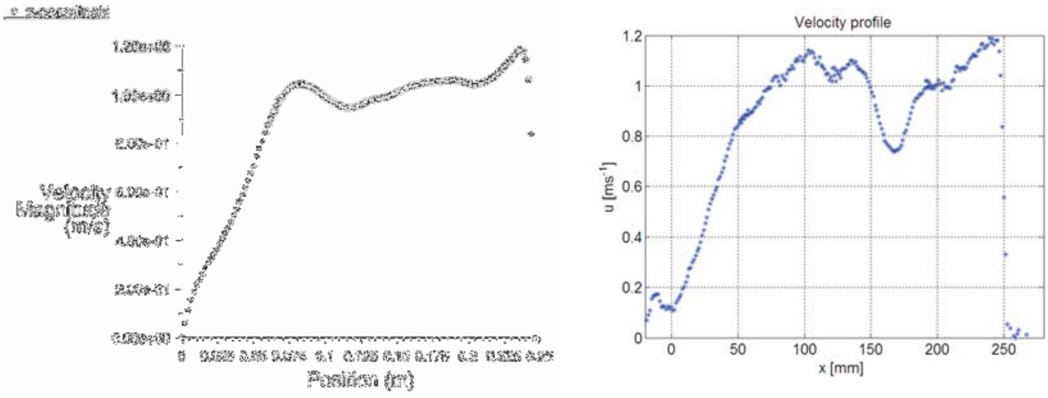

Figure 5 Velocity profile of the inlet nozzle, left - CFD model, right - PIV measurement

Due to the fact that data processing of the velocity profile is computantionally demanding, the measured area has been divided into severel segments. The velocity profile has been measured in each of these segments using a portable camera. The measurement results obtained are shown in Fig. 5 - right. Comparing both profiles, it is well seen that the CFD model fits the experimental data very well (except the section between 150-200 mm). The results of simulation of this CFD model have been used to define the boundary conditions needed for CFD simulation of the flow patterns at the single seat without passenger described in the next subsection.

4.2 CFD model of the single seat without a passenger

In order to test the potential of the local air ventilation system to create a closed microenvironment pocket, an experimental set-up has been built; see the scheme in Fig. 6. The simple model of both the seat and the back of the seat in front of it has been built from the aluminium profiles. As can be seen, both the inlet and outlet nozzles are fixed in the back of the seat. Both the nozzles are connected via pipe-lines with independent ventilators. Via the ventilators, both inlet and outlet flow rate can be controlled continuously. In order to visualize the flow patterns in the seat area, a jet with visualization particles has been connected to the inlet nozzle pipe. Through the mirror, the measured area has been enlightened by a reflector. The seat area has been sequentially photographed by a digital camera. The flow patterns have been visualised by two PIV methods, helium bubbles and safex fog. The results of the experiments are shown in Fig. 7.

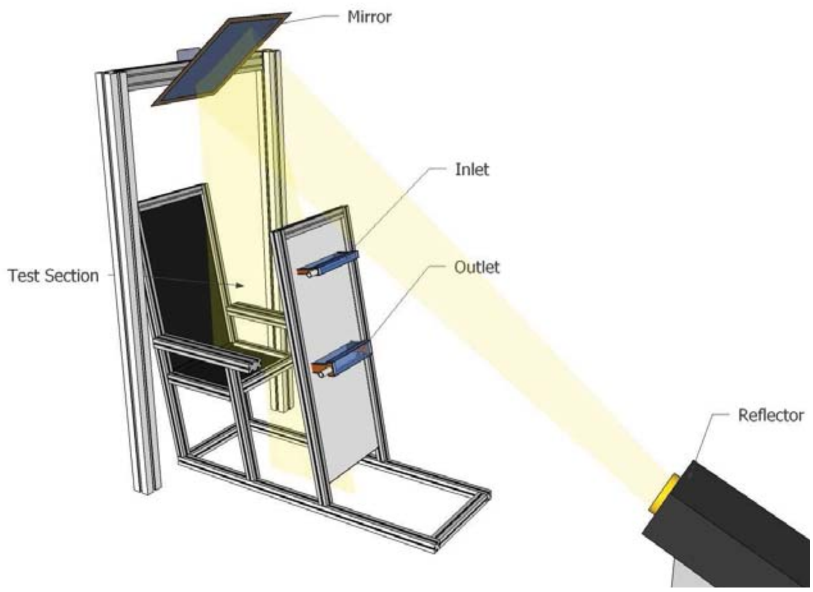

Figure 6 The experimental set-up for validation of the personalised ventilation

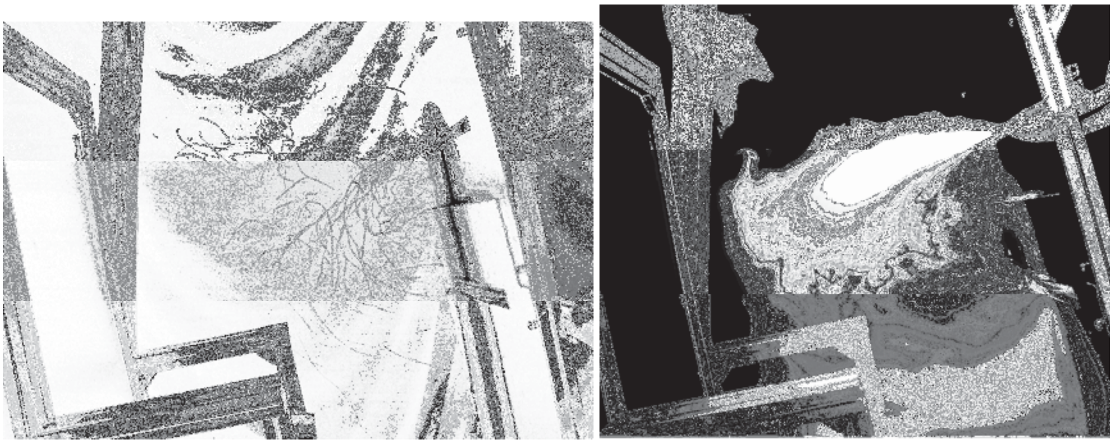

Figure 7 Visualization of the personalised ventilation, left - via helium bubbles, right - via Safex fog method

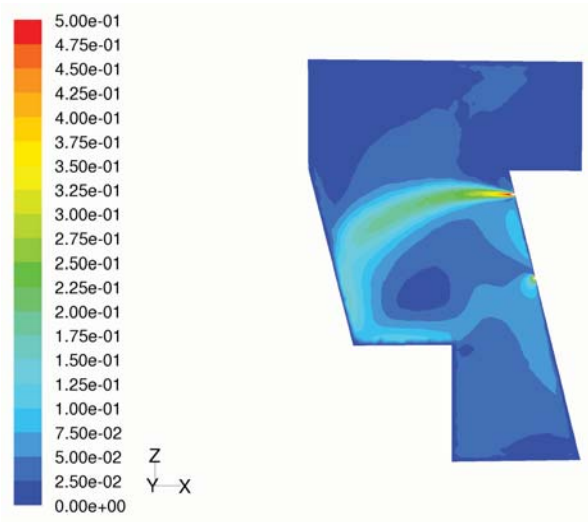

Figure 8 Velocity distribution in the CFD model of the experimental set-up

In order to compare the modelled and experimental data, a true 3D model of the experimental set-up has been built in the GAMBIT program. Consequently, the unstructured tetrahedral grid has been used for meshing this model. This kind of grid is necessary due to the complex geometry and finest grid near both nozzles. The average cell size is about 40 mm. Near the both nozzles the cell size is 5 mm. Then it gradually increases to 40 mm. The whole model consists of approximately 1 500 000 cells. For CFD simulation, the standard $k-\varepsilon$ model has been used as it was mentioned above. The results of the CFD model are shown in Fig. 8. As can be seen in both experiments in Fig. 7 and CFD model in Fig. 8, the desired flow patterns are obtained, starting at the inlet nozzle and ending at the outlet nozzle. Even though the velocity profiles have not been measured, it can be seen from the flow patterns that the experimental and simulated results are in a good agreement.

The model also showed the temperature sensitivity of the flow contours around the seat. The inlet air is to be maintained necessarily at temperature sufficiently lower than that in cabin interior. This is the prerequisite for directing the air flow from the inlet towards the outlet nozzle and for the consequent separation of the particular personalized air circulation from the other ones.

5 CFD models of personalized air distribution system

In order to obtain CFD models as close to reality as possible, a sufficiently detailed models of various cabin sectors have been developed. The geometrical data of the seats and of the cabin have been taken from Airbus A320. Also an adequately detailed model of the passenger's body has been compiled and placed on the seats. Three particular outputs from the models, namely, the air velocity, humidity and temperature distributions were followed and evaluated.

5.1 Humidification of the whole cabin volume

The first CFD model experiments with air humidification consider that the whole amount of the fresh air which enters the cabin is humidified, as it is shown in Fig. 9. As can be seen, the outside air supplied from the air conditioning pack is humidified and then mixed with the filtered recirculated air in the mixing manifold. Finally, the mixed air is supplied to the cabin via the central system. CFD studies of this humidification set-up have revealed its surprising disadvantages. First of all, as the whole cabin is to be humidified, the water consumption is higher than it is necessary for the passengers needs. However, above all, as can be seen from CFD results shown in Fig. 9, the air humidity turns out to be strikingly unevenly distributed over the cabin space if the humidification is provided through the central ventilation. Let us remark that the required relative humidity of the cabin air was considered 20%. As can be seen, the most humid air is distributed in the area above the aisle, while the least humid air is distributed around passengers seated by the cabin walls. In fact, according to the results of CFD, only those passengers who are seated by the aisle, take advantage of increased level of relative humidity distributed via the central system.

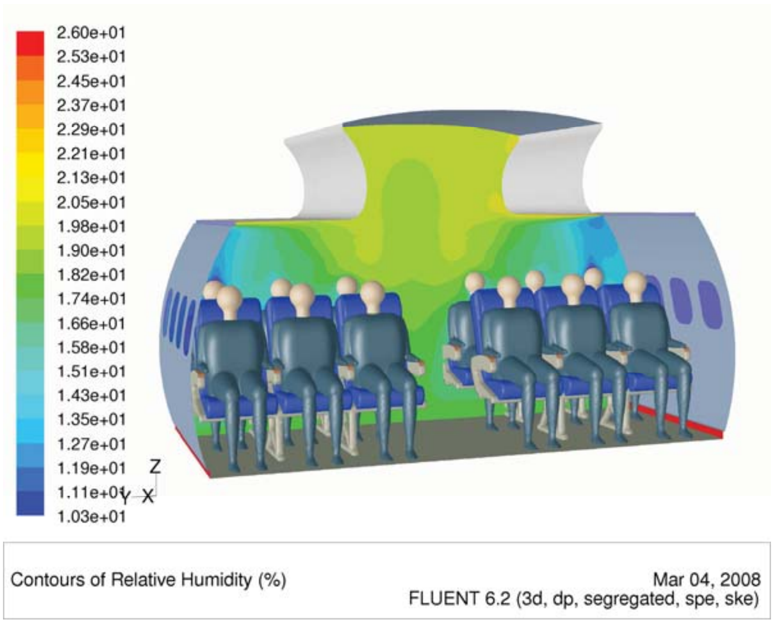

Figure 9 Relative humidity distribution resulting from the CFD model for the set-up – humidification of the whole cabin volume via central air distribution system

5.2 Personalized humidification by local air circulation driven from the backseat ahead

In the second stage, CFD models of the personalized ventilation system, described in section 2, are used to design the local circulation around the seat. The results are shown in Fig. 10, left – the velocity vector field, right – relative humidity distribution. The model experiments confirmed the feasibility of the local circulation driven from the nozzles built in the back seat ahead.

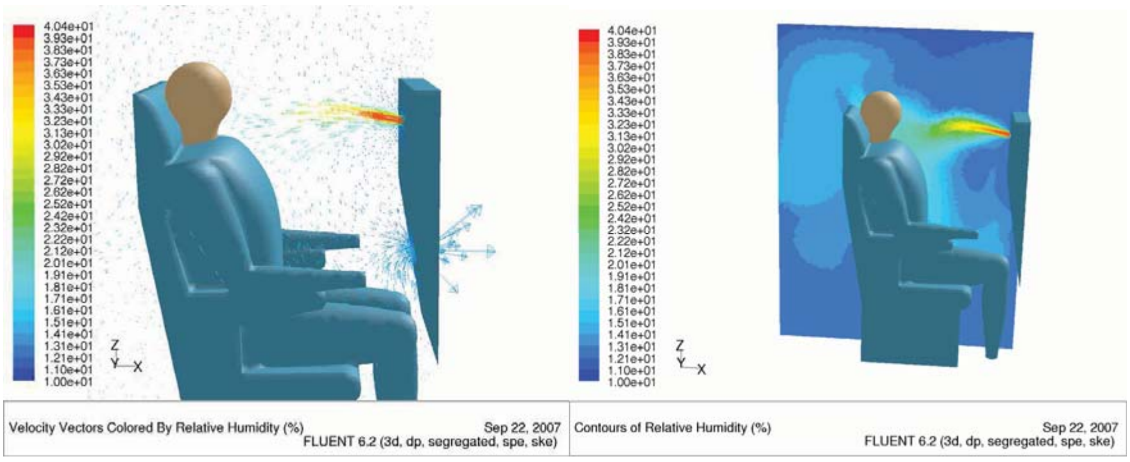

Figure 10 Air velocity and relative humidity visualization in the personalized local-air distribution system.

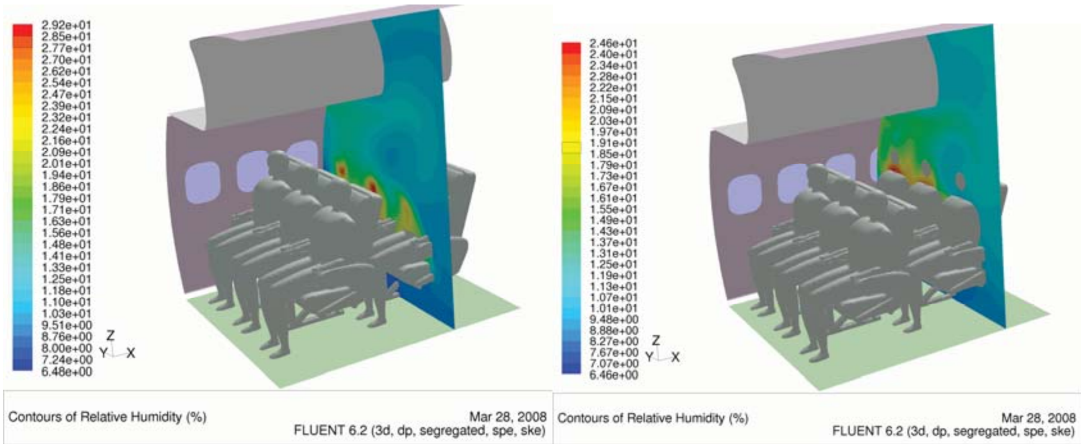

Figure 11 Distribution of the relative humidity in the seat area controlled by the personalized humidified-air distribution system with a local *air circulation driven from the backseat ahead*

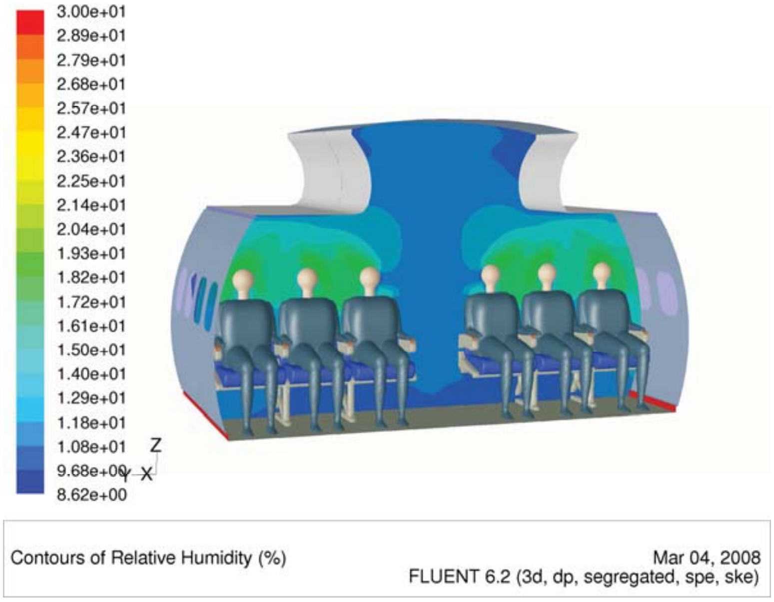

Figure 12 Relative humidity distribution resulting from the CFD model for the designed personalized humidification

In Fig. 11 and Fig. 12, the humidity distributions in the cabin are shown. Comparing them with Fig. 10, one can see the significant improvement of humidity distribution with respect to the passengers' breathing area.

As it has been proved on the circulation models, this design with properly adjusted nozzles and air velocities can supply the passenger with fresh and well humidified air as well as comply. As can be seen in the circulation patterns in Fig. 10 and Fig. 11, the micro-environment in the front of each of the passengers is separated from the other and maintained on improved humidity. When seated the passenger breathes "his/her own air" almost without any sharing it with the neighbours. In mounting the nozzles at the seat the designer has to respect the possibility of changing the position of the back-seats. Hence the nozzles have to be placed in a revolving manner, compensating their direction in case of the back-seat positioning.

6 Conclusions

At first the objective of the presented research was to provide higher humidity inside the airplane cabin during the transcontinental flights. However, the investigations made on CFD models very early discovered the fact that the cabin humidification provided via the centralized ECS leads to undesirable patterns of humidity distribution over the cabin volume, where most of the added moisture is spread near the cabin walls and corners. The role of the model was decisive in the research. From the CFD model experiments with varying the air flows focused on the seated manikins it turned out that it is possible to provide each passenger with "his/her own" fresh air despite one half of the air supply is re-circulated.

The proposed modification of the environmental control system would be beneficial for both the passenger health and comfort. On the other hand, in order to accomplish the personalized local-air distribution system described above, a considerable modification of the standard Environmental Control System needs to be performed. Namely, the following design issues need to be solved and adopted: redesigning the air conditioning pack, designing the air humidification system, designing the local air-distribution pipelines in the cabin floor and seats and reducing the performance of the central-air distribution system due to the air supplied by the local-air distribution system.

Acknowledgement: The presented research results have been achieved in the framework of the Project SEAT (Smart technologies for stress free air travel) sponsored by the European Commission DG H.3 Research, Aeronautics Unit under the 6th Framework Programme under contract Number: AST5-CT-2006-030958.

7 References

[1] Committee on Air Quality in Passenger Cabins of Commercial Aircraft, Board on Environmental Studies and Toxicology and National Research Council (2002), *The Airliner Cabin Environment and the Health of Passengers and Crew*, National Academy Press, Washington D.C

[2] Zhang, T., Q. Y. Chen, Novel Air Distribution Systems for Commercial Aircraft Cabins, *Building and Environmen*t, 42, 1675–1684, (2007).

[3] Penot, F., P. Meyer, Thermal and dynamic study of a new concept of HVAC system using an annular air jet, 7th International Conference on Air Distribution in Rooms: *Air distribution in rooms*, (2000).

[4] BRE - British Research Establishment. *Study of Possible Effects on Health of Aircraft Cabin Environments-Stage 2*. British Research Establishment, Environment Division, Garston, Watford, UK. 2001.

[5] Fluent 6.2 User's Guid, Fluent Inc, 2005

[6] Launder, B. E., D. B. Spalding. *Lectures in Mathematical Models of Turbulence*, Academic Press, London, England, 1972.

[7] Henkes, R. A. W. M, F. F. van der Flugt, and C. J. Hoogendoorn. Natural Convection Flow in a Square Cavity Calculated with Low-Reynolds-Number Turbulence Models. *Int. J. Heat Mass Transfer*, 34,1543-1557, (1991).

[8] Eng W, Harada L. and Jagerman L. (1982) The wearing of hydrophilic contact lenses aboard a commercial jet aircraft. *Aviat. Space Environ. Med.* Vol. 53, No. 3, pp. 235 – 238

[9] Haghighat F., Allard F., Megri A.C., Blondeau P. and Shimotakara R. (1999) Measurement of Thermal Comfort and Indoor Air Quality Aboard 43 Flights on Commercial Airlines. *Indoor Built Environment*, Vol. 8, pp. 58 – 65.